

# Effect of Loop Shape on the Drag-Induced Lift of Fly Line

Caroline Gatti-Bono

e-mail: gattic@umich.edu

Applied Numerical Algorithms, Computational Research Division, Lawrence Berkeley National Laboratory, Berkeley, CA 94720

N. C. Perkins

e-mail: ncp@umich.edu

Mechanical Engineering, University of Michigan, Ann Arbor, MI 48109-2125, Fellow ASME

*This note explains why casting a loop with a positive angle of attack is advantageous in distance fly casting. Several loop shapes, one with a positive angle of attack, one with a negative angle of attack, and two symmetrical loops with zero angle of attack are studied. For each loop, we compute the vertical drag component, i.e., the “lift.” It is found that a loop with a positive angle of attack generates lift about four times larger than a symmetrical loop. Thus, loops with positive angles of attack stay “aerIALIZED longer” which is consistent with observations made by (competition) distance fly casters. [DOI: 10.1115/1.1778414]*

## 1 Introduction

Fly casting involves considerable mechanics of both the fly rod and fly line as described in several studies, [1–9]. For instance, the angler imparts both rigid and flexible body motions of the fly rod in accelerating the fly line during the forward and back casting strokes. These strokes end with an abrupt deceleration of the fly rod, often referred to as the “stop,” after which a “loop” of fly line is formed as shown in the photograph below. This loop propagates as a nonlinear wave under the action of fly line tension, air drag and gravity. The initial conditions that form the initial shape and velocity of this loop are generated during a short time interval following the stop, [10]. Eventually the loop propagates to the end of the fly line and the attached “leader” and “fly” turn over as the line straightens at the end of the cast.

The dynamics of this loop is the subject of a number of studies beginning with those that assume idealized semi-circular or square loop shapes, [1–3]. Further studies, [5–9], relax these assumptions and compute the loop shape from the kinematics of the attached fly rod and the equations of motion of the flexible fly line. Fly casting experts (see, for example, [11–13]) are fully aware that the shape of the loop has considerable influence on its dynamics. For instance, it is well understood that loops with smaller diameters propagate farther as they provide less projected area in the flow, hence less air drag. As a result, casting small loops are a distinct advantage when casting longer distances or into a head wind.

The purpose of this note is to explain a second advantage that results from casting loops that are asymmetrical and with a positive angle of attack such as shown in Fig. 1. Fly casting loops of this form have a “pointed” top portion followed by a larger and more rounded “belly” beneath. The belly forms a positive angle of attack in the flow and the air drag along this portion of the loop generates a component that is vertically upwards. The upward drag component acts opposite gravity and allows these loops to

propagate farther. Fly casters sometimes say these loops “stay aerIALIZED” longer and also use the term “climbing loops” to describe this effect. The purpose of this note is to explain this observed phenomenon by analyzing the drag on a loop as a function of its shape. Below, we consider four qualitatively distinct loop shapes and compare their vertical drag components.

## 2 Analysis of Loop Drag

Four loop shapes are illustrated in Fig. 2. These loops have identical length  $l = \pi R$  and diameter  $2R$ , and are assumed to propagate to the right without changing shape. Two loops are asymmetrical (Figs. 2(a) and 2(b)) and two are symmetrical (Figs. 2(c) and 2(d)). The first asymmetrical loop (Fig. 2(a)) has a positive angle of attack and is termed a “climbing loop,” while the second (Fig. 2(b)) has a negative angle of attack and is termed a “falling loop.” The two symmetrical loops consist of a “pointed loop” and a “circular loop” as illustrated in Figs. 2(c) and 2(d), respectively. It should be noted that the shapes of these loops do not satisfy the steady-state conditions. However, they are close to the shapes observed in real casts and, therefore, they do provide good insight into the mechanics of a cast. Below we demonstrate how the loop shape significantly affects the vertical component of drag on fly line. We begin by computing the velocity field for an arbitrary loop shape.

**2.1 Velocity Field.** Figure 3 illustrates an arbitrary loop shape and a control volume that travels with the loop with velocity  $\mathbf{v}_{cv} = v_{cv}\mathbf{i}$ . The upper portion of the loop (assumed horizontal) travels with velocity  $\mathbf{v}_o = v_o\mathbf{i}$  and the velocity of the bottom portion of the loop (assumed horizontal) is zero as it is attached to the end of the stationary fly rod (and the effects of gravity are neglected). The velocity of an arbitrary material point P relative to the control volume is denoted as  $\mathbf{v}_r$  and its magnitude is uniform along the loop since the loop does not deform as it propagates. The absolute velocity of point P is

$$\mathbf{v}_p = \mathbf{v}_{cv} + \mathbf{v}_r \quad (1)$$

The velocities of the material points coincident with the top point (AA) and bottom (point BB) of the loop are

$$\mathbf{v}_{AA} = v_o\mathbf{i} \quad (2)$$

$$\mathbf{v}_{BB} = \mathbf{0}, \quad (3)$$

respectively. Using Eqs. (2) and (3) in Eq. (1) leads to the conclusion that

$$v_{cv} = v_r = \frac{v_o}{2} \quad (4)$$

Therefore,

$$\mathbf{v}_p = \frac{v_o}{2}\mathbf{i} + \frac{v_o}{2}\mathbf{e}_t \quad (5)$$

where  $\mathbf{e}_t$  is the unit tangent vector to the loop at P. Thus, given the shape of the loop, Eq. (5) can be used to evaluate the velocity of an arbitrary material point. Resolving this velocity into components tangential and normal to the loop allows one to compute the drag components due to skin friction and form drag as follows.

**2.2 Vertical Drag Component.** The drag on an element of fly line derives from skin friction (tangent to the element) and form drag (normal to the element). The drag coefficients for skin friction and form drag are denoted by  $C_{df}$  and  $C_{dn}$ , respectively. Let  $\rho_a$  denote the density of air and let  $d$  denote the diameter of the fly line (considered uniform for this example).

The loops shown in Fig. 2 are composed of straight segments and circular segments that, in total, subtend a semi-circle. For a straight segment of length  $l_s$ , the vertical component of drag is

Contributed by the Applied Mechanics Division of THE AMERICAN SOCIETY OF MECHANICAL ENGINEERS for publication in the ASME JOURNAL OF APPLIED MECHANICS. Manuscript received by the ASME Applied Mechanics Division, August 28, 2003; final revision, December 16, 2003. Associate Editor: O. M. O'Reilly.

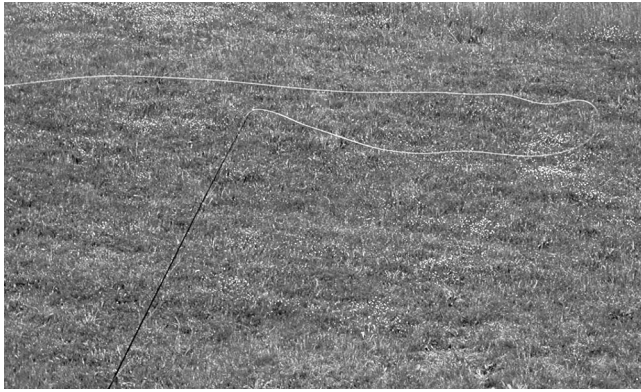


**Fig. 1** The fly line “loop” is formed after the “stop” in a casting stroke and propagates as a nonlinear wave. This loop is asymmetrical and possesses a positive angle of attack. Such loops are a hallmark of expert fly casters.

$$D_Y = -\frac{1}{2} \rho_a \pi dl_s C_{dt} v_t |v_t| \mathbf{e}_t \cdot \mathbf{j} - \frac{1}{2} \rho_a dl_s C_{dn} v_n |v_n| \mathbf{e}_n \cdot \mathbf{j} \quad (6)$$

where  $v_t$  and  $v_n$  are the velocity components tangential and normal to the fly line, respectively (see, for example, [14]). Note the contributions of both skin friction and form drag to this result. For the (sum of) circular segments of radius  $R$ , the vertical component of drag is

$$D_Y = \int_0^\pi \left[ -\frac{1}{2} \rho_a \pi d R C_{dt} v_t |v_t| \mathbf{e}_t \cdot \mathbf{j} - \frac{1}{2} \rho_a d R C_{dn} v_n |v_n| \mathbf{e}_n \cdot \mathbf{j} \right] d\theta$$

$$= \frac{\pi}{3} \rho_a d R v_o^2 C_{dt} \quad (7)$$

and this drag contribution depends only on the skin friction. We now employ Eqs. (6) and (7) to compute the vertical drag component for the four loops of Fig. 2.

**Climbing Loop:** For this loop, the straight segment  $CD = (\pi^2 + 4/4\pi)R$  and the semi-circle of radius  $R/2$ , composed of the arcs BC and DE, are subject to drag. The total drag is expressed as

$$D_Y = \frac{1}{2} \rho_a d R v_o^2 \left( \frac{(\pi^4 + 8\pi^2 + 64)\pi}{3(\pi^2 + 4)^2} C_{dt} + \frac{\pi(\pi^2 - 4)}{(\pi^2 + 4)^2} C_{dn} \right) \quad (8)$$

and the contribution due to form drag on the straight segment (second term) is positive due to the positive angle of attack (Fig. 2(a)).

**Falling Loop:** For this loop, the straight segment  $BC = (\pi^2 + 4/4\pi)R$  and the semi-circle of radius  $R/2$ , composed of the arcs AB and CD, are subject to drag. The total drag is expressed as

$$D_Y = \frac{1}{2} \rho_a d R v_o^2 \left( 4\pi \frac{(\pi^4 + 2\pi^2 + 4)}{3(\pi^2 + 4)^2} C_{dt} - \frac{\pi(\pi^2 - 4)}{(\pi^2 + 4)^2} C_{dn} \right) \quad (9)$$

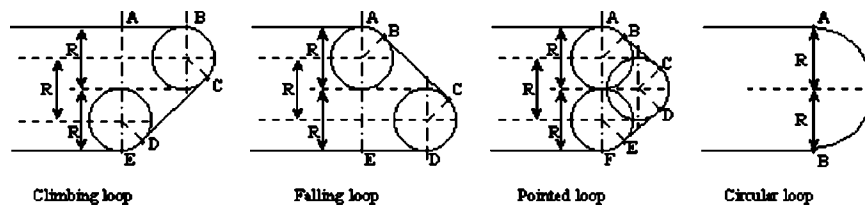


**Fig. 2** Four qualitatively different loop shapes. (a) and (b)  $l = AE$ , (c)  $l = AF$ , and (d)  $l = AB$

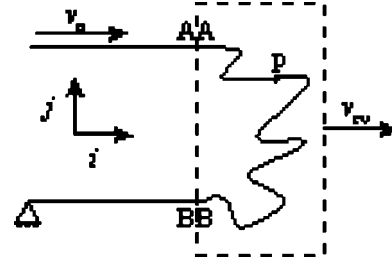


**Fig. 3** Kinematics of arbitrary loop

and the contribution due to form drag on the straight segment (second term) is negative due to the negative angle of attack (Fig. 2(b)).

**Pointed Loop:** For this loop, the straight segments  $BC = DE = \pi R/4$  and the semi-circle of radius  $R/2$ , composed of the arcs AB, CD, and EF, are subject to drag. The total vertical drag becomes

$$D_Y = \frac{1}{16} \rho_a d R v_o^2 \left( \frac{14\pi}{3} + \frac{2\pi(\pi^2 - 4)}{\pi^2} \right) C_{dt} \quad (10)$$

and the contributions due to form drag cancel due to symmetry.

**Circular Loop:** The result for this loop follows directly from Eq. (7)

$$D_Y = \frac{\pi}{3} \rho_a d R v_o^2 C_{dt} \quad (11)$$

and it is independent of form drag as mentioned above.

### 3 Example and Conclusions

Prior studies of fly line dynamics have used slightly different values for drag coefficients for skin friction and form drag, [1–3,5–9]. Here, we shall assume values  $C_{dt} = 0.015$  and  $C_{dn} = 1$  that are typical of those used in prior studies. We also recognize that these values depend, in general, on fly line speed (Reynold’s number), [2]. Using these drag coefficients and the results above leads to the following table that compares the lift on the four loops shown in Fig. 2.

The results of Table 1 show that the lift generated by a climbing loop is approximately *four times greater* than that of a semi-circular loop with the same characteristic dimensions. The source of this additional lift is the contribution of form drag on the “belly” of the fly line that has a positive angle of attack. The negative angle of attack for the falling loop shape results in a net negative “lift,” again due to the form drag on the belly. The symmetrical loops (circular and pointed) generate approximately the same lift. These results may be readily generalized to other loops shapes.

This note explains a fact observed by fly casting experts, namely, that a climbing loop is advantageous in distance casting. How to generate a climbing loop through control of the casting stroke is left as a (considerable) exercise to the reader.

**Table 1 Comparison of the vertical component of drag for the four loops shown in Fig. 2.**

	Climbing loop	Falling loop	Pointed loop	Circular loop
$\frac{16D_y}{\rho_a d R v_o^2}$	0.924	-0.450	0.276	0.251

### Acknowledgment

The authors wish to acknowledge the input of Mr. Bruce Richards from Scientific Anglers (3M) who first posed this interesting question to us.

### References

[1] Spolek, G. A., 1986, "The Mechanics of Flycasting: The Fly Line," *Am. J. Phys.*, **54**(9), pp. 832–835.  
 [2] Lingard, S., 1988, "Note on the Aerodynamics of a Fly Line," *Am. J. Phys.*, **56**(8), pp. 756–757.  
 [3] Robson, J. M., 1990, "The Physics of Flycasting," *Am. J. Phys.*, **58**(3), pp. 234–240.

[4] Hoffmann, J. A., and Hooper, M. R., 1998, "Fly Rod Response," *J. Sound Vib.*, **209**(3), pp. 537–541.  
 [5] Hendry, M. A., and Hubbard, M., 2000, "Dynamic Finite Element Simulation of Fly Casting and Its Potential Use in Fly Rod Design," *Proceedings: The Engineering of Sport*, Blackwell Science, London, pp. 407–414.  
 [6] Gatti-Bono, C., and Perkins, N. C., 2002, "Physical and Numerical Modelling of the Dynamic Behavior of Fly Line," *J. Sound Vib.*, **255**(3), pp. 555–577.  
 [7] Watanabe, T., and Tanaka, K., 2002, "Modelling the Dynamics of a Fly Line," *Proceedings The Engineering of Sport*, Blackwell Science, London, pp. 353–359.  
 [8] Gatti-Bono, C., and Perkins, N. C., 2003, "Comparison of Numerical and Analytical Solutions for Fly Casting Dynamics," *J. Sports Eng.*, **6**(3), pp. 165–176.  
 [9] Gatti-Bono, C., and Perkins, N. C., 2003, "Numerical Model for the Dynamics of a Coupled Fly Line/Fly Rod System and Experimental Validation," *J. Sound Vib.*, in press.  
 [10] Perkins, N. C., and Richards, B., 2003, "Dissecting Your Casting Stroke," *Fly Fisherman*, Primedia Magazines, Dec.  
 [11] Krieger, M. K., 1987, *The Essence of Flycasting*, Club Pacific, San Francisco, CA.  
 [12] Wulff, J., 1987, *Fly Casting Techniques*, The Lyons Press, Guilford, CT.  
 [13] Kreh, B., 1991, *Modern Fly Casting Method*, Odysseus Editions, Birmingham, AL.  
 [14] Sarpkaya T., and Isaacson M., 1981, *Mechanics of Wave Forces on Offshore Structures*, Van Nostrand Reinhold, New York.